Ab initio Studies of Ionization Potentials of Hydrated Hydroxide and Hydronium

Charles W. Swartz[1] and Xifan Wu[1,2,*]

[1]*Department of Physics, Temple University, Philadelphia, Pennsylvania 19122, USA*
[2]*Institute for Computational Molecular Science, Temple University, Philadelphia, Pennsylvania 19122, USA*

(Received 4 June 2013; published 20 August 2013)

The ionization potential distributions of hydrated hydroxide and hydronium are computed with the many-body approach for electron excitations with configurations generated by *ab initio* molecular dynamics. The experimental features are well reproduced and found to be closely related to the molecular excitations. In the stable configurations, the ionization potential is mainly perturbed by solvent water molecules within the first solvation shell. On the other hand, electron excitation is delocalized on both proton receiving and donating complex during proton transfer, which shifts the excitation energies and broadens the spectra for both hydrated ions.

DOI: 10.1103/PhysRevLett.111.087801 PACS numbers: 61.25.Em, 71.15.Pd, 79.60.−i, 82.30.Rs

The nature of the solvation structures of hydroxide (OH^-) and hydronium (H_3O^+) aqueous solutions is of fundamental interest. It is the prerequisite to understanding the mechanism of proton transfer (PT) through the autoprolysis process in water, which is behind diverse phenomena in physics, chemistry, and biology [1–7]. Photoemission spectroscopy (PES) has recently emerged as an important experimental technique in elucidating the interactions between hydrated ions and surrounding water molecules [6,8–10]. The state-of-the-art PES measurement is now able to measure the energy required to remove an electron from the solvated ions with respect to the Fermi level, which has been successfully used to determine the ionization potentials (IPs) of hydrated OH^- and H_3O^+ [6]. To have an insightful understanding of the experiments, there is a critical need for theoretical modeling, at the atomic scale, which can unambiguously connect the IP and its distributions to its solvation structures.

Given that the disordered structures of the liquids can be simulated by *ab initio* molecular dynamics (AIMD) [11,12], the PES spectra can be computed by the electron excitation theory such as Hedin's *GW* self-energy approximation [13,14]. However, such a theoretical approach has not yet been applied to the study of the PES spectra in ion solutions. The difficulty lies in the fact that the quasiparticle method scales unfavorably with the system size [14]. On the other hand, a proper simulation of disordered liquid structure requires a large supercell modeling. The computational burden is even more severe when it is necessary to take into account the statistical fluctuations of solvation structures both from the underlying H-bond network and, more drastically, from the structural diffusion of PT. As a compromise, the computationally efficient static density functional theory (DFT) [15] or the semiclassical approximation was used [6]. However, the static DFT designed for ground state electron minimization strongly underestimates the IP as an electron excitation property [6,14,15]. Because of the same difficulty, the precise assignment of IPs for these hydrated ions has yet not been accurately determined.

To address the above issues, in the current work, we generate the liquid structures of solvated hydroxide and hydronium in water by AIMD simulations and then compute the PES spectra within many-body formalism for electron excitation. In particular, we adopt a recently implemented methodology treating the inhomogeneous electronic screening of the medium [16–19], in which the maximally localized Wannier functions [20] are used to greatly increase the computational efficiency. The IPs of hydrated hydronium and hydroxide are determined by the real-space projection of the quasiparticle density of states on these solvated ion complexes. The resulting IPs and their distribution are in quantitative agreement with experiments in both position and broadening. The IPs of hydrated ions in liquid solutions are associated with the molecular excitation, however, strongly influenced by the water molecules in the first solvation shell. During the PT, the structural diffusion results in a delocalized defect eigenstate. As a result, the IPs of hydrated ions are broadened and shift into the main feature of bulk water. To the best of our knowledge, this is the first time that *GW* based quasiparticle theory has been applied to the PES spectra of ion solutions.

Ion solutions are generated by two equilibrated AIMD trajectories containing either one hydroxide or hydronium with 63 surrounding water molecules [21]. An elevated temperature of $T = 330$ K is used, which has been found to approximately capture the structural softening of a H bond in liquid water due to the quantum nuclear effect [24]. Electron excitation calculations are completed using the static Coulomb hole and screened exchange approach combined with electron screening effects from the inhomogeneous medium within the Hybertsen-Louie ansatz [16–19], in which the experimental dielectric constant of liquid water $\epsilon_0 = 1.8$ [25] is used as an input parameter.

In Fig. 1, we present our theoretical PES spectra of both ion solutions based on a quasiparticle density of states.

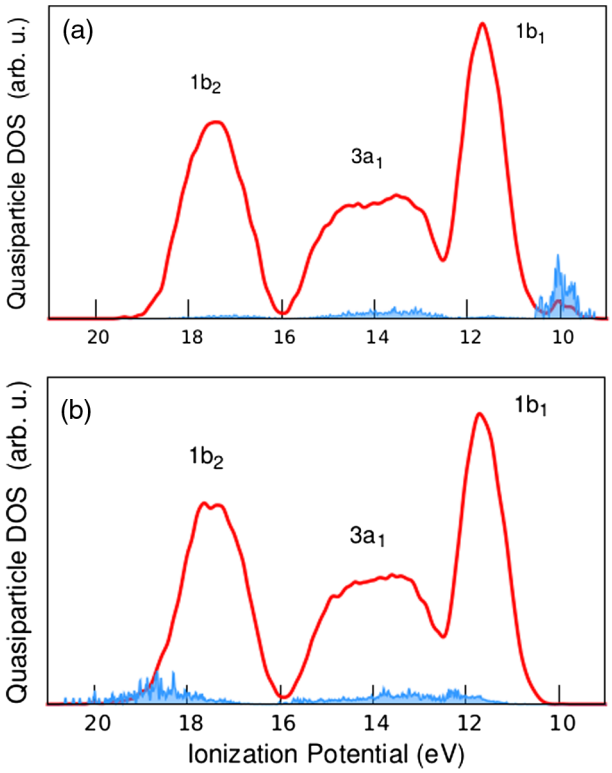

FIG. 1 (color online). Theoretical PES spectra (solid red lines) for the (a) OH^- and (b) H_3O^+ ion solutions. The shaded blue area indicate the IP of hydrated OH^- and H_3O^+ [26].

It can be seen that the overall PES spectra of both hydronium and hydroxide solutions are dominated by three features belonging to bulk water, which have $1b_2$, $3a_1$, and $1b_1$ characteristics with decreasing excitation energy as shown in Figs. 2(a)–2(c), respectively. The IP is associated with the valence electron excitation of a solvated ion in water. Although embedded in the water solution PES spectra, it still can be identified by the real-space projection of the quasiparticle density of states onto the hydrated ions in the energy range [26]. The resulting IP distributions of hydrated hydroxide and hydronium are also shown in the shaded areas of Figs. 1(a) and 1(b), respectively. It can be seen that the main feature of the IP of hydrated OH^- is represented by a narrow distribution, whose peak is centered at 9.99 eV and close to the low energy edge of the $1b_1$ feature of bulk water. The spectrum signal is much less obvious in the $3a_1$ region and almost absent in the $1b_2$ region of bulk water. As far as the IP of hydrated H_3O^+ is concerned, the most prominent feature is a broad peak centered at 19.01 eV close to the high energy edge of the $1b_2$ feature of bulk water. Much less signal is found in the $3a_1$ region, and almost no signal is found in the $1b_1$ region of bulk water. Strikingly, current theory accurately reproduces the experimental measurement [6], in which the IPs of hydrated hydroxide and hydronium are found to be centered at ~9.2 and ~20 eV, respectively. In both experiment [6] and current theory, the spectrum distribution of solvated hydronium is found to be much broader than that of solvated hydroxide. In stark contrast, the previous studies based on DFT calculations revealed that the IPs of solvated OH^- and H_3O^+ were located at ~12 and ~5 eV, respectively, which underestimated the experimental value over 50% [15]. This is because DFT, as a ground state theory, strongly underestimates the optical band gap properties. For a direct comparison with PES experiments, the electron excitation process can be more appropriately described by the *GW* self-energy approximation [27].

The accurate quasiparticle predictions now enable a more precise assignment of the IPs of hydrated ions. In Fig. 2, we present the representative quasiparticle wave

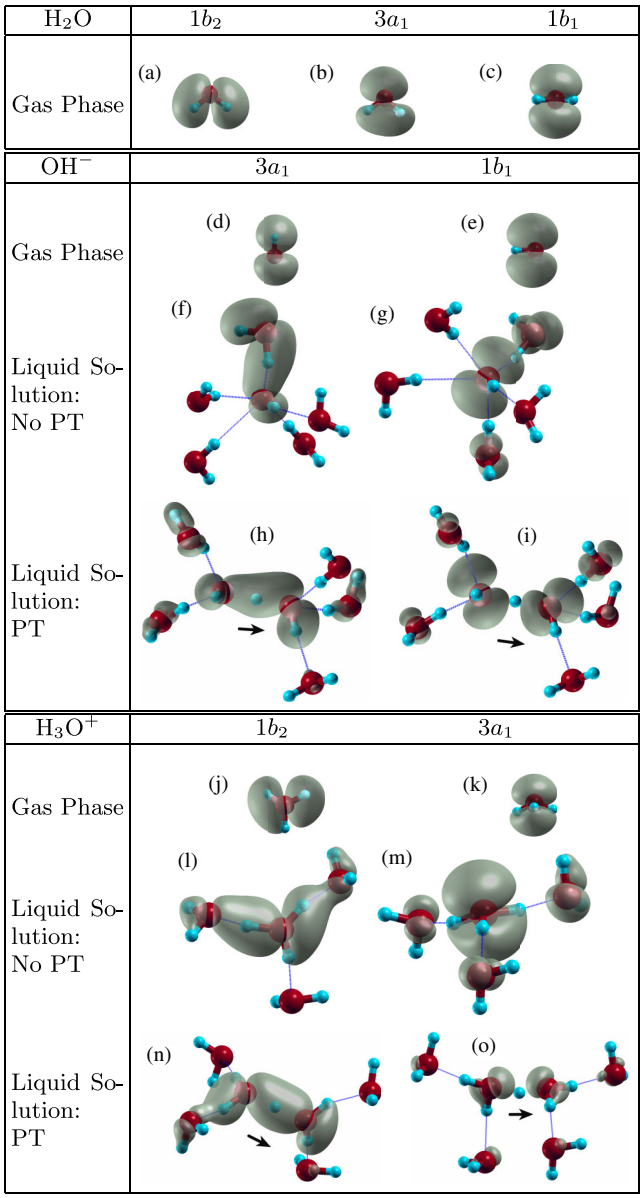

FIG. 2 (color online). QWs shown for the gas phase (a)–(c) H_2O, (d), (e) OH^-, and (j), (k) H_3O^+. Typical main feature $3a_1$ and $1b_1$ QWs displayed for hydrated OH^- in liquid solution while (f), (g) in a non-PT complex and (h), (i) during a PT. Similar $1b_2$ and $3a_1$ QWs are displayed for hydrated H_3O^+ while (l), (m) in the Eigen complex and (n), (o) in the Zundel complex.

functions (QWs) for the main features, which are located close to the $1b_1$ region of bulk water for hydrated OH^- and close to the $1b_2$ region of bulk water for hydrated H_3O^+. The typical QWs of less prominent features are also shown in Fig. 2, whose energies are in the $3a_1$ region of bulk water for both ion solutions. For comparison, the three lowest IP energy states of the OH^- and H_3O^+ monomers are also presented. The similarity of the electron excitation in ion solutions and that in gas phases indicates that the IPs should be attributed to molecular ionization, however, strongly perturbed by the solvation structures of the surrounding water molecules.

Clearly, the main feature of the IP in hydrated hydroxide at 9.99 eV should be assigned to the first valence electron excitation of the OH^- monomer. This is due to the resemblance of the electron excitations between the gas phase and the liquid solution. In the aqueous solution, the typical QW of the main feature is a well-localized hydroxide defect state of clear lone pair character, as shown in Figs. 2(g) and 2(i). It originates from two degenerate 1π bonds of the OH^- monomer. The degeneracy is broken by the disordered liquid structure and results in an excitation distribution instead of one single ionization energy. It can be expected that the spectrum distribution is largely dependent on the solvation structure and will be different with or without PT. In the absence of PT, the current AIMD simulation finds that solvated hydroxide adopts the most stable configuration in such a way that OH^- accepts four H bonds with the possibility of donating one [1]. The four water molecules donating the H bond are approximately in one plane. Consistently, this lone pair QW is mainly localized on the OH^- itself, however, with a significant weight on the water molecules within the first solvation shell. Thus, without PT, the IP is mainly affected by the fluctuating first-shell solvation structure embedded in the H-bond network of liquid water. During PT, the OH^- exchanges one proton with a neighboring water molecule. Our current simulation indicates that the PT mechanism is consistent with the dynamical hypercoordination scenario proposed by Tuckerman *et al.* [1]. The structural diffusion is initiated by breaking one of the four accepting H bonds and followed by a proton exchange along the shortest H bond. Intriguingly, the structural diffusion is accompanied by a nontrivial change in the electronic state. The lone pair QW is now localized on both proton donating and proton receiving molecules, as shown in Fig. 2(i), instead of its main localization on OH^- only before the PT in Fig. 2(g). The delocalized QW facilitates its hybridization with surrounding water molecules. As a result, the IP exhibits a blueshift towards the main feature of the bulk water spectra accompanied by a broadened distribution as illustrated in Fig. 3(a).

In a similar scenario, we assign the main feature of the IP distribution of hydrated hydronium to the second valence excitation of two degenerate p orbitals of the H_3O^+ monomer. The degeneracy is again broken by the disordered molecular environment. Without PT, the excited QW has a similar characteristic as the $1b_2$ orbital in liquid water and is mainly localized on the so-called Eigen complex (H_3O^+), as shown in Fig. 2(l). In particular, a large orbital amplitude is also found on the three water molecules along the direction of donated H bonds by H_3O^+. The QW then decays rapidly to zero in the second solvation shell and beyond. As a result, the excitation is a hydronium defect state with $1b_2$ character that is localized on the $H_9O_4^+$ complex, which is also the so-called strongly solvated Eigen cation [28]. In the process of PT, the current simulation is consistent with the widely accepted Grottuss diffusion mechanism [1]. The proton exchange takes place by the interconversion between the Eigen and Zundal ($H_5O_2^+$) complex [1]. Not surprisingly, the locality of the QW also swifts from the Eigen to the Zundal complex during PT, as shown in Figs. 2(l) and 2(n), respectively. Interestingly, a significant weight is also found to be centered on the transferring proton connecting both the proton receiving and donating structures, which gives a unique signal for PT in the electronic structure. Similar to the PT process of hydrated OH^-, the delocalized H_3O^+ defect state is much more easily hybridized with solvent H_2O molecules. As a result, in Fig. 3(b), we observe a redshift of the IPs into the $1b_2$ region of bulk water which gets broadened simultaneously.

Interestingly, a comparison of the IPs between these two ion solutions reveals that the main feature of hydrated H_3O^+ has a much broader distribution than that of OH^-. We attribute it to the difference in orbital characters. For the hydrated H_3O^+ excitation with the $1b_2$ characteristic, the covalent orbital on an OH bond is easily perturbed by the H-bond network of liquid water. On the other hand, the excitation of hydrated OH^- is of lone pair character and only centered on oxygen atom, which will be much less affected by the embedded H-bond network. This is also consistent with the observation that the $1b_1$ peak is also narrower than the $1b_2$ peak in liquid water [29].

Besides the main features, the excitations of hydrated ions are also found in Fig. 1 within the $3a_1$ region of bulk water for both solutions. However, the signals are much weaker and broadly distributed. Nevertheless, the IPs of hydrated ions should still be assigned to the molecular excitation of the same $3a_1$ symmetry, which are the second and first excitation of OH^- and H_3O^+ monomers, respectively. In Figs. 4(a) and 4(d), we present the typical QW densities of $3a_1$ excitations as a function of distance from the solvated OH^- and H_3O^+, respectively. For comparison, the same quantities of the main feature are also shown in Figs. 4(b) and 4(c). Clearly, in both ion solutions, the less prominent IPs of $3a_1$ character originate from relatively delocalized QWs, in which a large orbital amplitude falls into the second solvation shell and beyond. On the contrary, QWs of the main features of both hydrated ions are defect states strongly localized within the first solvation shell. As a result, the total integrated charge density converges to one electron much more rapidly as a function of increased distance from the ions, as shown in

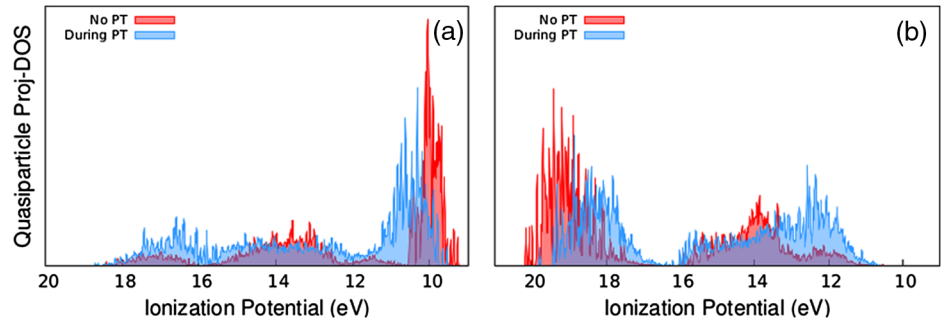

FIG. 3 (color online). Theoretical IP distributions for hydrated (a) OH^- and (b) H_3O^+. The red and blue areas denote the stable configurations and those configurations currently experiencing a PT, respectively [39].

Figs. 4(b) and 4(c). The delocalized QWs indicate a stronger hybridization with the water solution and result in the observed broader and weaker ion excitations.

Finally, we draw our attention to the energy range where the least IP signals have been found. They are the $1b_2$ and $1b_1$ regions of bulk water for hydrated OH^- and H_3O^+, respectively. Again, this can be understood by the symmetry of electron excitation of both ions at the monomer level. The electronic configurations of OH^- and H_3O^+ ions are intrinsically different from that of a single water molecule. For the OH^- monomer, the three lowest allowed valence excitations are the two degenerated excitations of $1b_1$ character, followed by one of $3a_1$ character, in which the $1b_2$-like orbital in water is not allowed by symmetry. On the other hand, the three lowest valence excitations in H_3O^+ ions are ones with $3a_1$ character, followed by two degenerate states with $1b_2$ character, in which a $1b_1$ orbital is forbidden. These symmetry restrictions result in the absence of electron excitation for hydrated ions in the above energy range.

In conclusion, the IP distributions of hydrated OH^- and H_3O^+ are studied by accurate quasiparticle theory. The excitations of solvated ions can be assigned to molecular electron excitation, however, strongly perturbed by the solvation structures. Although the main features of IPs are determined by their stable configurations, the proton transfer does introduce a change of position and distributions of electron excitation in both hydrated ions. We suggest that the excitation change due to PT can be detected by isotope effects in future PES measurements on solvated H_3O^+ and D_3O^+ [30]. Finally, we comment that the leftover mismatch between experiment and theory could be further reduced by more accurate liquid structures considering both dispersion force [31–33] and

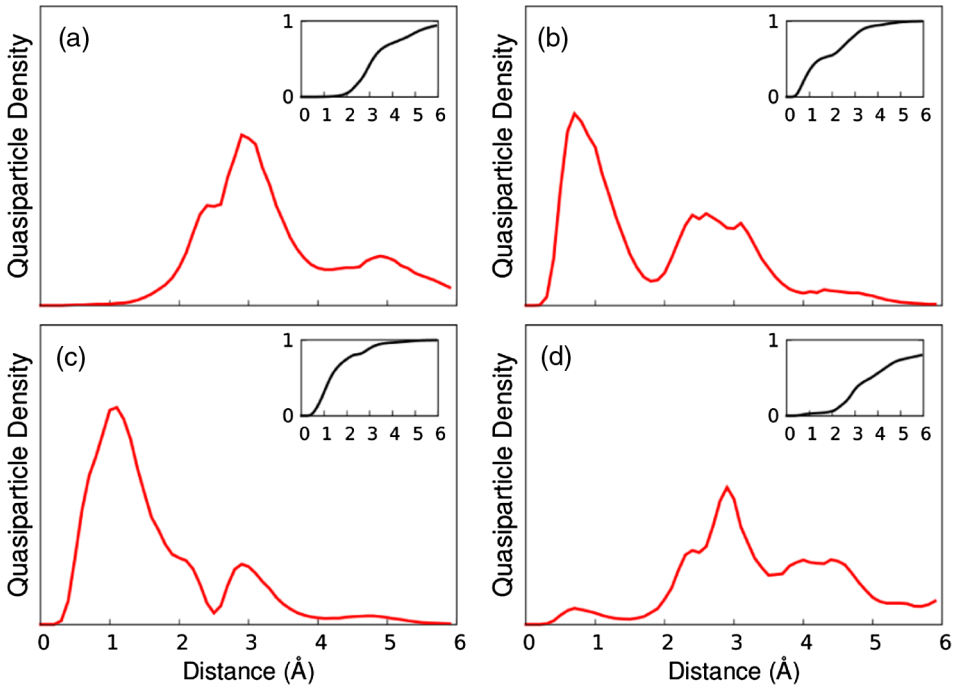

FIG. 4 (color online). Typical QW densities (arbitrary units) for hydrated OH^- characteristic states, (a) $3a_1$ and (b) $1b_1$, and hydrated H_3O^+ characteristic sates, (c) $1b_2$ and (d) $3a_1$, as a function of distance from O^* [26]. The insets show the total integrated density.

self-interaction error correction in a DFT functional [34,35] and by including frequency dependence of excitation beyond static *GW* [36–38].

X. W. thanks Roberto Car for valuable discussions. This work is supported by the U.S. Department of Energy under Grant No. DE-SC0008726. Computational support is provided by the National Energy Research Scientific Computing Center and the National Science Foundation through TeraGrid resources provided by NICS under Grant No. TG-DMR120045.

*xifanwu@temple.edu

[1] D. Marx, A. Chandra, and M. K. Tuckerman, Chem. Rev. **110**, 2174 (2010).
[2] M. Tuckerman, A. Chandra, and D. Marx, Acc. Chem. Res. **39**, 151 (2006).
[3] A. Hassanali, M. K. Prakash, H. Eshet, and M. Parrinello, Proc. Natl. Acad. Sci. U.S.A. **108**, 20410 (2011).
[4] J. T. Hynes, Nature (London) **397**, 565 (1999).
[5] D. Asthagiri, L. Pratt, J. D. Kress, and M. Gomez, Proc. Natl. Acad. Sci. U.S.A. **101**, 7229 (2004).
[6] B. Winter, M. Faubel, I. Hertel, C. Pettenkofer, S. Bradforth, B. Jagoda-Cwiklik, L. Cwiklik, and P. Jungwirth, J. Am. Chem. Soc. **128**, 3864 (2006).
[7] A. Chandra, M. E. Tuckerman, and D. Marx, Phys. Rev. Lett. **99**, 145901 (2007).
[8] B. Winter, R. Weber, I. V. Hertel, M. Faubel, P. Jungwirth, E. C. Brown, and S. E. Bradforth, J. Am. Chem. Soc. **127**, 7203 (2005).
[9] B. Winter, R. Weber, W. Widdra, M. Dittmar, M. Faubel, and I. V. Hertel, J. Phys. Chem. A **108**, 2625 (2004).
[10] R. Weber, Ph.D. thesis, Freie Universita, 2003.
[11] R. Car and M. Parrinello, Phys. Rev. Lett. **55**, 2471 (1985).
[12] P. H.-L. Sit, C. Bellin, B. Barbiellini, D. Testemale, J.-L. Hazamann, T. Buslaps, N. Marzari, and A. Shukla, Phys. Rev. B **76**, 245413 (2007).
[13] L. Hedin, Phys. Rev. **139**, A796 (1965).
[14] G. Onida, L. Reining, and A. Rubio, Rev. Mod. Phys. **74**, 601 (2002).
[15] M. Tuckerman, K. Laasonen, and M. Parrinello, J. Chem. Phys. **103**, 150 (1995).
[16] M. S. Hybertsen and S. G. Louie, Phys. Rev. B **37**, 2733 (1988).
[17] X. Wu, A. Selloni, and R. Car, Phys. Rev. B **79**, 085102 (2009).
[18] W. Chen, X. Wu, and R. Car, Phys. Rev. Lett. **105**, 017802 (2010).
[19] L. Kong, X. Wu, and R. Car, Phys. Rev. B **86**, 134203 (2012).
[20] N. Marzari, A. A. Mostofi, J. R. Yates, I. Souza, and D. Vanderbilt, Rev. Mod. Phys. **84**, 1419 (2012).
[21] A periodic cubic cell corresponding to the experimental ambient density of water is used. Both simulations are preceded by a 3 ps equilibrium run and then continued over a 25 ps time scale within the canonical ensemble. The atomic force is calculated by DFT using the PBE functional [22] with a kinetic energy cutoff of 70 Ry. All calculations are performed using the QUANTUM-ESPRESSO code package [23].
[22] J. P. Perdew, K. Burke, and M. Ernzerhof, Phys. Rev. Lett. **77**, 3865 (1996).
[23] P. Giannozzi, P. Baroni, N. Bonini, M. Calandra, R. Car, C. Cavazzoni, D. Ceresoli, G. L. Chiarrotti, M. Cococcioni, and I. Dabo, J. Phys. Condens. Matter **21**, 395502 (2009).
[24] Z. Li, Ph.D. thesis, Princeton University, 2012.
[25] G. P. Johari and S. J. Jones, Proc. R. Soc. A **349**, 467 (1976).
[26] Individual IPs were calculated by projecting the QWs onto a real-space sphere of 1.5 Å [15] centered on the O^* atom while in a stable complex and centered on the transferring proton during PT. Configurations are considered to be in a proton transfer event when a single H^+ could not be associated with any oxygen molecules. The IPs of hydrated ions are amplified by a factor of 10 in order to increase their visibility. The identities of both the OH^- and the H_3O^+ are determined by counting the number of H^+ inside a covalent radius of 1.17 Å for each oxygen atom in a given configuration. Those oxygens containing one or three H atoms within their covalent radius are referred to as O^* and determine both OH^- and H_3O^+, respectively.
[27] We want to stress here that the IPs for both solvated ions are averaged over 100 configurations, weighted to include both PT and non-PT configurations, and sampled during the 25 ps equilibrium trajectory. PT configurations account for ~10% of the total OH^- configurations and ~16% of the H_3O^+ configurations.
[28] B. Kirchner, ChemPhysChem **8**, 41 (2007).
[29] D. Prenergast, J. Grossman, and G. Galli, J. Chem. Phys. **123**, 014501 (2005).
[30] D. Marx, M. Tuckerman, J. Hutter, and M. Parrinello, Nature (London) **397**, 601 (1999).
[31] C. Zhang, J. Wu, G. Galli, and F. Gygi, J. Chem. Theory Comput. **7**, 3054 (2011).
[32] B. Santra, J. Klimeš, D. Alfé, A. Tkatchenko, B. Slater, A. Michaelides, R. Car, and M. Scheffler, Phys. Rev. Lett. **107**, 185701 (2011).
[33] R. A. DiStasio, O. Anatole von Lilienfeld, and A. Tkatchenko, Proc. Natl. Acad. Sci. U.S.A. **109**, 14791 (2012).
[34] C. Zhang, T. A. Pham, F. Gygi, and G. Galli, J. Chem. Phys. **138**, 181102 (2013).
[35] C. Zhang, D. Donadio, F. Gygi, and G. Galli, J. Chem. Theory Comput. **7**, 1443 (2011).
[36] W. Kang and M. S. Hybertsen, Phys. Rev. B **82**, 195108 (2010).
[37] D. Lu, F. Gygi, and G. Galli, Phys. Rev. Lett. **100**, 147601 (2008).
[38] The static *GW* is found to slightly overestimate the IP [14,36], which can be corrected by frequency dependence in the *GW* method.
[39] Those configurations where the hydrated ion is not experiencing a PT (in its stable configuration) are defined by $\delta > 0.6$ Å, and those configurations currently experiencing a PT are defined by $\delta \sim 0$ Å. In the above, δ is defined as $\delta = |R_{O^*H} - R_{O_wH}|$, where R_{O^*H} and R_{O_wH} are the distances between a shared proton and O^* [26] or a surrounding water molecule's oxygen, respectively. The minimum δ value for a particular O^* is considered most likely to produce a PT, and $\delta = 0$ indicates that the shared proton is halfway between two molecules [2].